

# Detection of Amine Vapors using Luminescent Xerogels from Supramolecular Metal-Containing Gelator

Junpei Sasaki,<sup>1</sup> Masahiro Suzuki,<sup>2</sup> Kenji Hanabusa<sup>\*2,3</sup>

<sup>1</sup> Faculty of Textile Science & Technology, Shinshu University, Ueda, 386-8567 Japan

<sup>2</sup> Interdisciplinary Graduate School of Science & Technology, Shinshu University, Ueda, 386-8567 Japan

<sup>3</sup> Division of Frontier Fibers, Institute for Fiber Engineering, ICCER, Shinshu University, Ueda, 386-8567 Japan



E-mail: hanaken@shinshu-u.ac.jp

Kenji Hanabusa

## Abstract

Supramolecular fluorescent gelators containing a tris( $\beta$ -diketonato) complex are synthesized by using gelation-driving chelates, and their gelation abilities are studied with 15 solvents. Thin-layer films are prepared on quartz plates from the solutions and they are studied as chemosensors for amines. Fluorescence-quenching of the thin-layer films upon exposure to saturated primary and secondary amine vapors is monitored to evaluate the abilities of the chemosensors to detect amines. The morphologies of the thin-layer films are observed by Transmission electron microscopy (TEM) and discussed in relation to their fluorescence-quenching. The fluorescence-quenching efficiencies upon exposure to saturated primary and secondary amines depend on the basicity and bulkiness of the amines rather than the vapor pressure. The fluorescence-quenching is caused by decomposition of a complex through nucleophilic addition of primary or secondary amines to its carbonyl group. The detection of tertiary amines is performed by monitoring the fluorescence emission from the thin-layer films, which are composed of a ligand and EuCl<sub>3</sub>. The emergence of fluorescence originates from the formation of fluorescent Eu<sup>3+</sup>-containing gelator, in which dehydrochloric acid by tertiary amines is a trigger for the complexation

## 1. Introduction

The detection of organic amines in a trace vapor sample has received and continues to receive considerable attention because these are widely used in food industries, gas treatment plants, and pharmaceutical production<sup>1</sup> in spite of the fact that low-molecular-weight amines are toxic and easily absorbed by the body. Much research has been devoted to developing sensors for amines in solutions;<sup>2</sup> however, studies on solid-state sensors for detecting amines have been reported only in a limited number of papers.<sup>3-14</sup>

High surface-to-volume ratios, which facilitate the sensing of analytes adsorbed on their surfaces, are indispensable in developing solid-state sensors. The adsorption of sensing molecules on supports with a high surface area requires a high surface-to-volume ratio; for instance, microcrystalline cellulose,<sup>7</sup> filter paper,<sup>11</sup> porous polymers,<sup>9</sup> and TLC<sup>13</sup> were used as supports. Amorphous sensing materials are also useful for developing solid-state sensors, because such compounds can form amorphous structures with high surface areas without

crystallization. Calixarene derivatives,<sup>3-5</sup> triphenylamine derivatives,<sup>6,14</sup> a bulky medium-sized molecule,<sup>8</sup> and a conjugated polymer<sup>12</sup> were reported as amorphous sensing materials. It is also noteworthy that a fibrous xerogel film prepared with gels formed using a gelator was firstly used as an amine sensor.<sup>10</sup> One of the noticeable features of gelators is their formation of gels with self-assembled fibers rather than crystals. As the xerogels derived from gels are composed of three dimensional fibrous networks with high surface-to-volume ratios, thin-layer films of xerogels are useful for sensor applications.

Over the last two decades, we have developed many low-molecular-weight gelators and proposed the concept of a “gelation-driving segment.” This gelation-driving segment is expected to be a useful tool for developing various types of gelators.<sup>15</sup> We prepared fluorescent gelators containing a gelation-driving segment and reported thin-layer xerogel chemosensors to detect explosives such as TNT and RDX by fluorescence-quenching.<sup>16,17</sup> In this paper, we report the synthesis of trifluoroacetylacetone-based metal-containing gelators, and we employ fibrous thin-layer films derived from the gelators as chemosensors for the detection of amines. Herein, we demonstrate two different procedures to detect amines; one is for detecting primary and secondary amines by monitoring fluorescence-quenching, while the other is for exclusively detecting tertiary amines by monitoring fluorescence emission

## 2. Experimental

### 2.1. Instrumentation

Elemental analysis was performed with a Perkin-Elmer 2400 IICNHS/O analyzer. Infrared spectra were recorded on a Jasco FS-420 spectrometer using KBr plate. Fluorescence spectra were recorded on a Jasco FP-6300 spectrometer. Transmission electron microscopy (TEM) and fluorescence microscopy (FM) were performed with a JEOL JEM-SS and an Axio Imager M1 microscope, respectively. <sup>1</sup>H NMR spectra were recorded on a Bruker AVANCE 400 spectrometer. Dynamic force mode (DFM) of scanning probe microscope was done with a SII SPA-4001. Wide angle X-ray diffraction (WAXD) was performed with a Rigaku Rotaflex RU-200B.

### 2.2. Gelation test

Gelation test was carried out by an upside-down test tube method. A typical procedure is as follows: A weighed sample and 1 mL of solvent in a septum-capped test tube with internal diameter of 14 mm was heated until the solid dissolved. The

resulting solution was cooled at 25°C for 2 h and then the gelation was checked visually. When no fluid ran down the wall of the test tube upon inversion of the test tube, we judged it to be gel. The gelation ability was evaluated by the minimum gel concentration of a gelator being necessary for gelation at 25°C. The unit is g L<sup>-1</sup> (gelator/solvent). The solvents used for gelation test were hexane, dodecane, cyclohexane, methanol, ethanol, 1-propanol, acetone, ethyl acetate, THF, 1,4-dioxane, DMF, DMSO,  $\gamma$ -BL ( $\gamma$ -butyrolactone), toluene, and chloroform.

### 2.3. Synthesis

**Compound 1:** A mixture of 21 mL (176 mmol) of ethyl trifluoroacetate, 18.4 g (135 mmol) of 4-hydroxyacetophenone, and 1.26 mL of ethanol was dissolved in 77 mL of dry DMF. To the reaction mixture, 12.7 g (317 mmol) of NaH (60 wt% oil) was added little by little at 0 °C. The reaction mixture was stirred for 2 h at room temperature, and then for 3 h at 35~40 °C. After adding crushed ice and 37 mL of 12 M HCl, the reaction mixture was extracted with ether and washed with water. The ether layer was dried with MgSO<sub>4</sub> and evaporated. The residue was recrystallized from a mixture of ligroin/THF (50 mL/80 mL). The sublimation at 110°C in vacuo (1 mmHg) of a crude product followed by recrystallization from a mixture of toluene/ligroin (80 mL/50 mL) provided the pure compound **1** in a yield of 15.7 g (50%). FT-IR (KBr); 3377 cm<sup>-1</sup> (v -OH, phenol), 1660 cm<sup>-1</sup>, 1600 cm<sup>-1</sup>, 1576 cm<sup>-1</sup> (v C=O, diketone), 1161 cm<sup>-1</sup> (v C-O,  $\delta$  -OH, phenol). Found: C 51.91, H 2.92%. Calcd for C<sub>10</sub>H<sub>7</sub>F<sub>3</sub>O<sub>3</sub>: C 51.74, H 3.04%. <sup>1</sup>H NMR (400 MHz, CDCl<sub>3</sub>, TMS, 25 °C)  $\delta$  = 7.90 (d, 2H, J = 8.8, Phe), 6.94 (d, 2H, J = 8.8, Phe), 6.50 (s, 1H, enol-OH), 2.59 (s, 1H, COCH/COH).

**Compound 2:** A mixture of 1.00 g (10 mmol) of succinic anhydride and 3.84 g (10 mmol) of L-isoleucylaminooctadecane<sup>16</sup> was added in 300 mL of dry CH<sub>2</sub>Cl<sub>2</sub> and stirred overnight at room temperature. The reaction mixture was evaporated and recrystallized from 450 mL of ethyl acetate to give 4.59 g (95%) of the compound **2**. FT-IR(KBr); 1707 cm<sup>-1</sup> (v C=O, carboxylic acid). Found: C 70.31, H 11.69, N 5.62%. Calcd for C<sub>28</sub>H<sub>54</sub>N<sub>2</sub>O<sub>4</sub>: C 69.66, H 11.27, N 5.80%. <sup>1</sup>H NMR (400 MHz, CDCl<sub>3</sub>, TMS, 25°C)  $\delta$  = 7.10 (d, 1H, J = 8.9, CONHCH), 6.23 (t, 1H, J = 5.6, CONHCH<sub>2</sub>), 4.21 (t, 1H, J = 8.4, CONHCH/CONH), 3.09-3.37 (m, 2H, CONHCH<sub>2</sub>), 2.64-2.74 (m, 2H, CH<sub>2</sub>CONH), 2.49-2.59 (m, 2H, HOOCCH<sub>2</sub>), 1.77-1.89 (m, 1H, CH(CH<sub>3</sub>)(CH<sub>2</sub>CH<sub>3</sub>)), 1.44-1.58 (m, 2H, CONHCH<sub>2</sub>CH<sub>2</sub>), 1.21-1.34 (m, 32H, alkyl, CH(CH<sub>3</sub>)(CH<sub>2</sub>CH<sub>3</sub>)), 0.84-0.94 (m, 9H, CH<sub>3</sub>).

**Compound 3:** A mixture of 1.00 g (4.31 mmol) of compound **1**, 2.08 g (4.31 mmol) of compound **2**, 0.544 g (4.31 mmol) of DiPC (*N,N'*-diisopropylcarbodiimide), 1.27 g (4.31 mmol) of DPTS (4-dimethylamino pyridinium *p*-toluenesulfonate) in 40 mL of dry CH<sub>2</sub>Cl<sub>2</sub> was stirred overnight at 40°C. The matter after evaporation was purified by recrystallization from 50 mL of ethanol followed by from a mixture of methanol/toluene (125 mL/25 mL). The compound **3** was obtained in a yield of 2.31 g (77%). FT-IR(KBr); 1761 cm<sup>-1</sup> (v C=O, ester). Found: C 65.96, H 9.04, N 4.44%. Calcd for C<sub>38</sub>H<sub>59</sub>F<sub>3</sub>N<sub>2</sub>O<sub>6</sub>: C 65.49, H 8.53, N 4.02%. <sup>1</sup>H NMR (400 MHz, CDCl<sub>3</sub>, TMS, 25°C)  $\delta$  = 7.97 (d, 2H, J = 8.8, Phe), 7.26 (d, 2H, J = 8.8, Phe), 6.54 (s, 1H, enol-OH), 6.34 (d, 1H, J = 8.7, CONHCH), 5.94 (t, 1H, J = 5.7, CONHCH<sub>2</sub>), 4.23 (dd, 1H, J = 7.0, 8.7, CONHCH/CONH), 3.10-3.34 (m, 2H, CONHCH<sub>2</sub>), 2.95 (t, 2H, J = 6.6, CH<sub>2</sub>CONH), 2.66 (s, 1H, COCH/COH), 2.50-2.73 (m, 2H, OCOCH<sub>2</sub>), 1.81-1.99 (m, 1H, CH(CH<sub>3</sub>)(CH<sub>2</sub>CH<sub>3</sub>)), 1.39-1.57 (m, 2H, CONHCH<sub>2</sub>CH<sub>2</sub>), 1.17-1.35 (m, 32H, alkyl, CH(CH<sub>3</sub>)(CH<sub>2</sub>CH<sub>3</sub>)), 0.83-0.96 (m, 9H, CH<sub>3</sub>).

**Compound 4:** A mixture of 1.12 g (2.0 mmol) of *N*-11-bromoundecanoylL-isoleucylaminooctadecane<sup>16</sup> and 0.464 g (2.0 mmol) of the compound **1** was dissolved in 30 mL of dry

DMF at 40°C. To the solution was added 0.386 g (2.8 mmol) of K<sub>2</sub>CO<sub>3</sub> and 0.332 g (2.0 mmol) of KI, followed by stirred at 40°C overnight under an argon atmosphere. The mixture was poured to iced water and acidified by conc. HCl. A precipitated matter was filtered off, washed with water, and dried. Recrystallization from ethanol gave the compound **4** in a yield of 1.11 g (71%). FT-IR (KBr); 1633 cm<sup>-1</sup> (vC=O, amide I), 1603 cm<sup>-1</sup> (vC=O, diketone). Found: C 69.19, H 10.29, N 3.69%. Calcd for C<sub>45</sub>H<sub>75</sub>N<sub>2</sub>O<sub>5</sub>: C 69.20, H 9.68, N 3.59%. <sup>1</sup>H NMR (400 MHz, CDCl<sub>3</sub>, TMS, 25 °C)  $\delta$  = 7.92 (d, 2H, J = 9.0 Hz, Phe), 6.97 (d, 2H, J = 9.0 Hz, Phe), 6.50 (s, 1H, enol-OH), 6.07 (d, 1H, J = 8.1 Hz, CONHCH), 5.87 (t, 1H, J = 6.0 Hz, CONHCH<sub>2</sub>), 4.19 (t, 1H, J = 8.1 Hz, CONHCHCONH), 4.04 (t, 2H, J = 6.5 Hz, OCH<sub>2</sub>CH<sub>2</sub>), 3.72 (q, 1H, J = 7.0 Hz, CH(CH<sub>3</sub>)(CH<sub>2</sub>CH<sub>3</sub>)), 3.14-3.35 (m, 2H, CONHCH<sub>2</sub>), 2.20 (t, 2H, J = 7.56 Hz, CH<sub>2</sub>CONH), 1.76-1.88 (m, 1H, COCH/COH), 1.41-1.57 (m, 2H, CONHCH<sub>2</sub>CH<sub>2</sub>), 1.20-1.39 (m, 48H, alkyl and CH(CH<sub>3</sub>)(CH<sub>2</sub>CH<sub>3</sub>)), 0.85-0.95 (m, 9H, CH<sub>3</sub>).

**Complex 5:** A solution of 2.00 g (2.87 mmol) of compound **3** in 50 mL of ethanol was added to a solution of 0.350 g (0.960 mmol) of europium (III) chloride hexahydrate and 440  $\mu$ L (3.16 mmol) of triethylamine in 10 mL of ethanol. The mixture was stirred for 2 h at 50°C, and then the resulting mixture was poured on a crushed ice. A precipitated matter was collected and recrystallized from a mixture of THF/hexane (60 mL/60 mL). The complex **5** was obtained in a yield of 1.76 g (77%). FT-IR(KBr); 1735 cm<sup>-1</sup> (v C=O, ester), 1636 cm<sup>-1</sup> (vC=O, amide I), 1542 cm<sup>-1</sup> (vC=O, diketone). Found: C 61.41, H 8.00, N 4.13%. Calcd for C<sub>114</sub>H<sub>174</sub>F<sub>9</sub>N<sub>6</sub>O<sub>18</sub>Eu: C 61.05, H 7.96, N 3.75%.

**Complex 6:** This compound was prepared from 0.150 g (0.645 mmol) of **1**, 0.0825 g (0.218 mmol) of europium (III) chloride hexahydrate, and 100  $\mu$ L (0.713 mmol) of triethylamine according to the same procedure described above. The recrystallization from a mixture of THF/hexane (10 mL/10 mL) gave 0.15 g (86%) of complex **6**.

**Complex 7-Eu:** A solution of 1.00 g (1.28 mmol) of compound **4** in 50 mL of ethanol was added to a solution of 0.17 g (0.47 mmol) of europium (III) chloride hexahydrate and 193  $\mu$ L (1.41 mmol) of triethylamine in 10 mL of ethanol. The mixture was stirred for 5 h at 50°C, and then the resulting mixture was poured on a crushed ice. A precipitated matter was collected and recrystallized from a mixture of THF/hexane (20 mL/20 mL). The complex **7-Eu** was obtained in a yield of 0.59 g (58%). Found: C 65.20, H 9.21, N 3.93%. Calcd for C<sub>135</sub>H<sub>222</sub>F<sub>9</sub>N<sub>6</sub>O<sub>15</sub>Eu: C 65.06, H 8.98, N 3.54%. FT-IR(KBr); 1635 cm<sup>-1</sup> (vC=O, amide I), 1599 cm<sup>-1</sup> (vC=O, diketone).

**Complex 7-Tb:** A solution of 0.438 g (0.561 mmol) of compound **4** in 30 mL of methanol was added to a solution of 0.140 g (0.374 mmol) of terbium (III) chloride hexahydrate and 156  $\mu$ L (1.41 mmol) of triethylamine in 10 mL of methanol. The mixture was stirred for 3 h at 50°C, and then the resulting mixture was poured on a crushed ice. A precipitated matter was collected and recrystallized from a mixture of THF/hexane (15 mL/25 mL). The complex **7-Tb** was obtained in a yield of 0.369 g (79%). FT-IR(KBr); 1635 cm<sup>-1</sup> (vC=O, amide I), 1600 cm<sup>-1</sup> (vC=O, diketone). Found: C 64.69, H 9.40, N 3.81%. Calcd for C<sub>135</sub>H<sub>222</sub>F<sub>9</sub>N<sub>6</sub>O<sub>15</sub>Tb: C 64.88, H 8.95, N 3.36%.

**Complex 7-Al:** This compound was prepared from 0.400 g (0.513 mmol) of compound **4** and 0.0455 g (0.342 mmol) of aluminum (III) chloride according to the same procedure described in complex **7-Tb**. A yield; 0.295 g (73%). FT-IR(KBr); 1635 cm<sup>-1</sup> (vC=O, amide I), 1600 cm<sup>-1</sup> (vC=O, diketone). Found: C 68.09, H 9.61, N 3.81%. Calcd for C<sub>135</sub>H<sub>222</sub>F<sub>9</sub>N<sub>6</sub>O<sub>15</sub>Al: C 68.50, H 9.45, N 3.55%.

### 2.4. Preparation of thin-layer films as sensors

Thin-layer films as chemosensor were prepared by

directly drop-casting method. A typical procedure is as follows: The warm DMSO solution of complex **5** (3  $\mu$ L of  $1.0 \times 10^{-3}$  M) was drop-casted on a quartz plate of 15W $\times$ 2D $\times$ 50H and dried in vacuum. Exposure to saturated amine vapor was done in a glass tube vessel with a diameter of 37 mm and a height of 110 mm, in the bottom of which an amine source was placed (Figure S1). Forty percent of methylamine solution in methanol and 25% of ammonia solution were used as their vapor sources. Aniline, butylamine, hexylamine, and 2-naphthylamine were used as they were. Thin-layer films for detecting tertiary amines were prepared as follows: The ligand **3** (0.696 mg, 1.0 mmol) and 0.366 mg (1.0 mmol) of europium (III) chloride hexahydrate was dissolved in 1 mL of DMSO and then 3  $\mu$ L of the resulting solution was drop-casted on a quartz plate of 15W $\times$ 2D $\times$ 50H and dried in vacuum.

### **3. Results and Discussion**

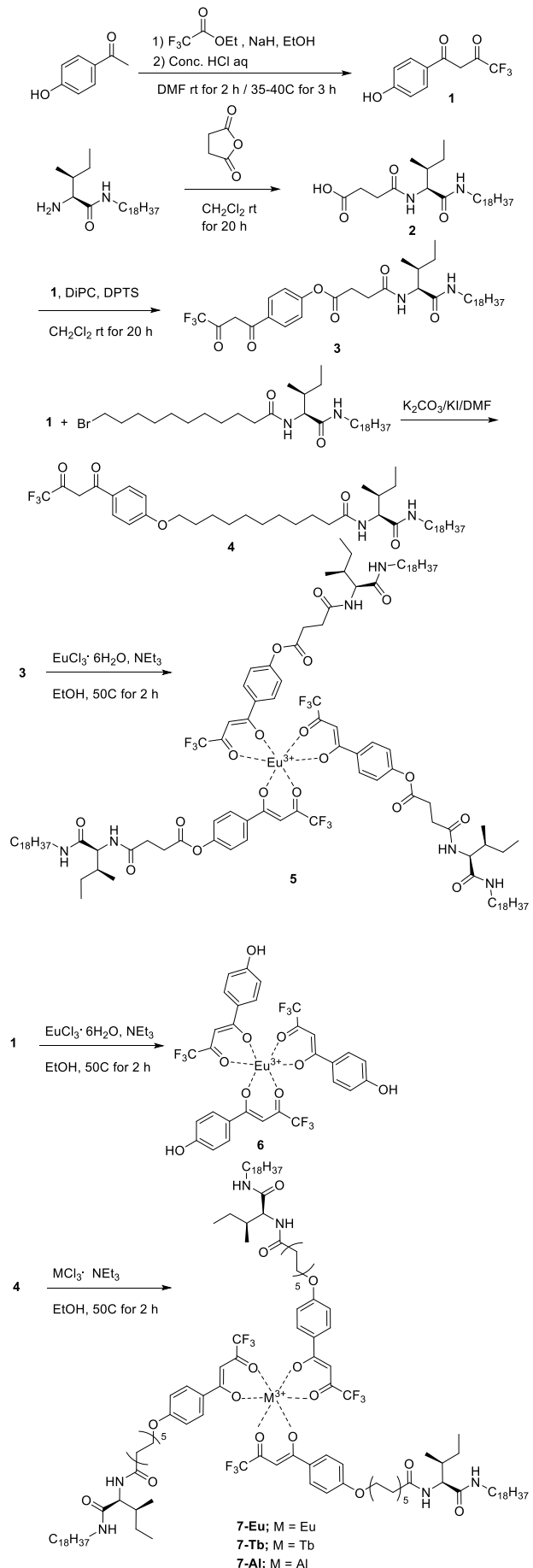
### **3.1. Gelation behavior of fluorescent metal-containing gelators**

Recently, several researchers have shown considerable interest in studying gelators that can physically gel fluids. Such gelators are of interest because they can immobilize substantial volumes of solvent. Many gelators have so far been reported<sup>18</sup> and information regarding their gelation-driving segments has been accumulated. Gelators of low-molecular-weight compounds are characterized by thermally reversible sol-gel transitions, because three-dimensional network structures are built up through noncovalent interactions such as hydrogen bonding, electrostatic interactions, van der Waals interactions, and  $\pi$ - $\pi$  interactions. To prepare gelators as ligands, we employed a gelation-driving segment based on L-isoleucine.<sup>16</sup> Chelate gelators (**3** and **4**) and fluorescent metal-containing gelators (complexes **5**, **7-Eu**, **7-Tb**, and **7-Al**) were prepared according to Scheme 1. Complex **6**, which had no gelation ability, was also prepared for comparison. Complexes **5**, **6**, and **7-Eu** are Eu<sup>3+</sup>-containing complexes, while **7-Tb** and **7-Al** contain Tb<sup>3+</sup> and Al<sup>3+</sup>, respectively. Gelation tests were performed using the upside-down test-tube method and their results for 15 solvents are summarized in Table 1, where solvents are placed in order of their dielectric constants. All the compounds were too soluble in chloroform and THF to act as gelators. Complex **6**, which is not included in Table 1, was miscible in solvents having a high polarity more than chloroform and almost insoluble in solvents that have low polarity than 1,4-dioxane. Chelates **3** and **4**, which were constructed from a gelation-driving segment of L-isoleucine, could gel 13 solvents but not chloroform and THF. In spite of the strong gelation behavior of **3** and **4**, their Eu<sup>3+</sup>-containing complexes (**5** and **7-Eu**) gelled only DMSO and resulted in "I" or "P" towards most solvents. The insolubility and precipitation of **3** and **4** could be due to the strong solvophobic character of their Eu<sup>3+</sup> complexes. Complex **7-Tb**, which was prepared from chelate **4** and terbium (III) chloride, could gel polar solvents, such as 1,4-dioxane, ethyl acetate, acetone, ethanol, methanol, DMF, DMSO, and  $\gamma$ -BL. Complex **7-Al** was an excellent gelator in terms of the number of solvents that could be gelled. Considering that the gelation ability of **7-Al** was equal to that of chelate **4**, its complexation with Al<sup>3+</sup> had a significant influence on the formation of three dimensional networks for gelation.

### **3.2. UV and fluorescence spectroscopy**

Fluorescence excitation spectra and emission spectra of thin-layer films of **5**, **6**, **7-Eu**, **7-Tb**, and **7-Al** are shown in Figure S2, where the thin-layer films were prepared by drop-casting 1 mM DMSO solutions onto quartz plates. The maximum excitations ( $\lambda_{ex}$ ) of **5**, **6**, **7-Eu**, **7-Tb**, and **7-Al** were

observed at 344, 370, 339, 342, and 348 nm, respectively.



**Scheme 1.** Synthetic routes for the complexes.

**Table 1.** Gelation test of chelates and metal-containing gelators at 25°C

Solvent	<b>3</b>	<b>4</b>	<b>5</b>	<b>7-Eu</b>	<b>7-Tb</b>	<b>7-Al</b>
Hexane	GTL (10)	GO (10)	I	I	P	GTL (10)
Dodecane	GT (4)	GO (10)	I	P	P	GTL (10)
Cyclohexane	GT (8)	GTL (10)	P	I	P	GT (20)
Toluene	GT (10)	GTL (40)	S	S	S	GT (20)
1,4-Dioxane	GO (20)	GTL (40)	PG	P	GO (40)	GTL (40)
Chloroform	S	S	S	S	S	S
Ethyl acetate	GO (8)	GTL (10)	S	I	GO (40)	GO (20)
THF	S	S	S	S	S	S
Acetone	PG	GTL (8)	P	I	GO (20)	GO (20)
1-Propanol	GTL (40)	GO (40)	P	P	PG	S
Ethanol	GO (40)	GO (40)	P	I	GO (40)	GO (20)
Methanol	GO (40)	GO (10)	I	I	GTL (20)	GO (20)
DMF	GTL (40)	GTL (10)	I	GTL (20)	GTL (10)	GT (20)
DMSO	GTL (20)	GTL (10)	GTL (20)	GTL (20)	GT (4)	GT (4)
$\gamma$ -BL	GTL (20)	GTL (8)	I	P	GT (10)	GTL (8)

GT: Transparent gel, GTL: Translucent gel, GO: Opaque gel, PG: Partial gel, I: Almost insoluble, P: Precipitation, S: Soluble,  $\gamma$ -BL:  $\gamma$ -Butyrolactone.

The values indicate the minimum gel concentrations at 25°C; the units are g L<sup>-1</sup> (gelator/solvent).

The wavelengths of the maximum emissions ( $\lambda_{em}$ ) of **5**, **6**, **7-Eu**, **7-Tb**, and **7-Al** were found at 613, 613, 614, 545, and 412 nm, according to their Stokes' shifts. The detection of amines was evaluated by monitoring the fluorescence-quenching of the aforementioned fluorescence  $\lambda_{em}$  peaks. We also studied the concentration dependence of the absorption spectra of solutions of **5** and **7**. Figure 1 shows the absorption spectra of **5**, **7-Eu**, and **7-Tb** in DMSO solutions at various concentrations. The wavelengths of the absorption maxima ( $\lambda_{max}$ ) of **5** were approximately constant at 380 nm regardless of the concentrations (Figure 1a), where the decrease in absorbance as the concentration increased was due to the formation of opaque gels. The  $\lambda_{max}$  of **7-Eu** exhibited a red-shift from 376 to 387 nm along with an increase in the concentration from 2.5 to 20 mg mL<sup>-1</sup> (Figure 1b). The  $\lambda_{max}$  of **7-Tb** also exhibited a red-shift from 364 to 376 nm accompanied by an increase in the concentration from 0.5 to 4.0 mg mL<sup>-1</sup> (Figure 1c). It should be mentioned that the minimum gel concentrations of **7-Eu** and **7-Tb** in DMSO are 20 and 4 mg mL<sup>-1</sup>, respectively. The slight decrease in absorbance in Figure 1b and Figure 1c is probably due to the light scattering of gels of **7-Eu** and **7-Tb**. The observed red-shift accompanied by an increase in the concentration suggests that there are interactions, such as J-aggregate formation, within complexes **7-Eu** and **7-Tb**. Since the decamethylene segments in **7-Eu** and **7-Tb** insulate the complex regions from the hydrogen bonding regions adjacent to the L-isoleucine residue, the complex regions may form J-aggregates without hindrance from the rigid intermolecular hydrogen bonding regions. In the case of **5**, the tris( $\beta$ -diketonato)europium region was fixed close to the hydrogen bonding region with a short ethylene segment; consequently, the rigidity of the hydrogen bonding regions will prevent J-aggregate formation.

### 3.3. Fluorescent sensors for detecting amines

Thin-layer sensors were prepared by directly drop-casting warm solutions onto quartz plates, followed by spin-coating and drying in vacuo. Physical gelation by gelators occurs via the self-aggregation of molecules driven by noncovalent bonding, resulting in the formation of fibrous aggregates. The fibrous aggregates ultimately form a 3D network structure; namely, nanosized fibrous aggregates predictably form during the initial stage of gelation. Therefore, it can be assumed that the fibrous

aggregates will be fixed in thin-layer films prepared from gelators. The high surface area resulting from the formation of fibrous aggregates is an advantage for sensor applications.

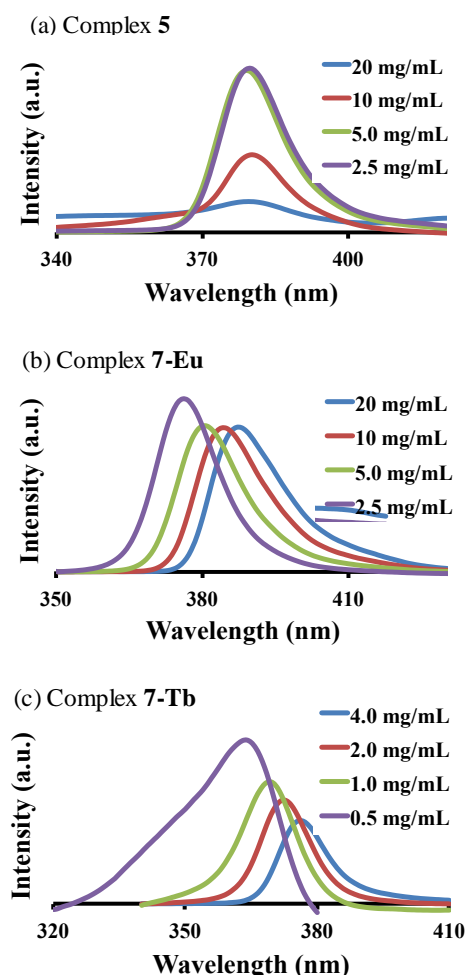


**Figure 1.** Absorption spectra of **5**, **7-Eu**, and **7-Tb** in DMSO solutions at various concentrations.

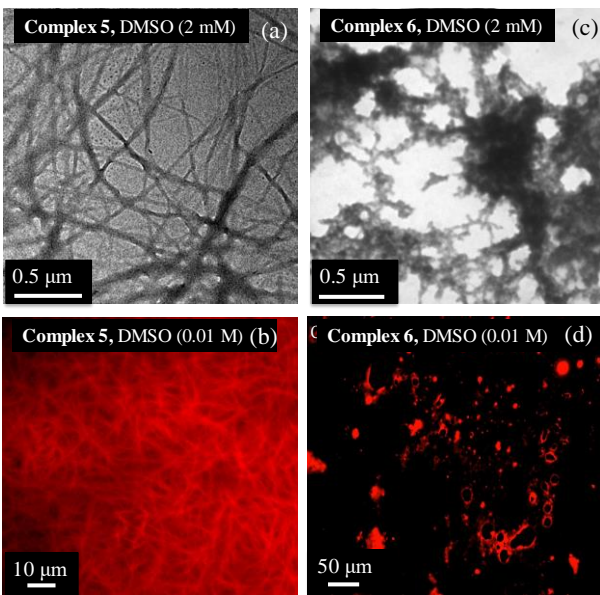


**Figure 2.** TEM and FM images.

- (a) TEM image of a xerogel prepared from DMSO gel of **5** (2 mM).
- (b) FM image of DMSO gel of **5** (10 mM).
- (c) TEM image of dried sample prepared from DMSO solution of **6** (2 mM).
- (d) FM image of DMSO solution of **6** (10 mM).

The fibrous aggregates fixed in thin-layer films; that is to say, the morphology of fibrous aggregates in xerogels, can be characterized by TEM. We also used FM, which enables direct observation of a wet gel containing solvent. Figure 2a shows a TEM image of a xerogel prepared from a warm DMSO solution of complex **5** (2 mM; 4.48 g L<sup>-1</sup>), in which fibrous aggregates of juxtaposed and interlocked fibers with widths ranging from 27 to 104 nm were observed. Figure 2b shows an FM image of a DMSO gel of **5** (10 mM; 22.4 g L<sup>-1</sup>). The FM image was constructed by monitoring the emission at 605~670 nm under excitation at 365 nm. Fibers with widths ranging from 0.83 to 2.5 μm were observed in the DMSO gel of **5** (Figure 2b). On the other hand, a TEM image of a sample prepared from a DMSO solution (2 mM; 1.69 g L<sup>-1</sup>) of complex **6**, which had no gelation ability, showed a gathering of nanoparticles, whose diameters ranged from 18 to 54 nm (Figure 2c). An FM image of a DMSO solution of **6** (10 mM; 8.45 g L<sup>-1</sup>) also confirmed microstructures with diameters of 5 to 20 μm (Figure 2d). The TEM and FM images clearly show that fibrous aggregates responsible for physical gelation were formed in a DMSO gel of complex **5**; on the contrary, nano- to micro-sized particles were observed in a DMSO solution of complex **6**. It can be expected that xerogel films prepared by drop-casting a warm DMSO solution of **5** will have a large surface area that can successfully make contact with amine vapors, resulting in effective quenching.

We compared the sensing abilities of thin-layer films prepared from **5** and **6**. Figure 3 shows the fluorescence-quenching efficiencies of the thin-layer films upon exposure to saturated vapors of ammonia and butylamine. These thin-layer films were prepared by dropping 3 μL of 1.0 mM DMSO solutions of each compound. The excitation wavelength was 344 nm and the fluorescence-monitoring wavelength was 613 nm. The fluorescence-quenching efficiencies of the thin-layer film of complex **5** were ~55% and 74% after exposure to ammonia for 10 and 30 min, respectively. On the contrary, the efficiencies of complex **6** were limited to ~15% and 46%, respectively. A similar tendency was observed with respect to the sensing abilities when the complexes were exposed to saturated

butylamine vapor (Figure 3b). The superiority of the sensing abilities of complex **5** is attributed to the fact mentioned above; namely, fibrous aggregates of juxtaposed and interlocked fibers were formed in thin-layer films of **5**.

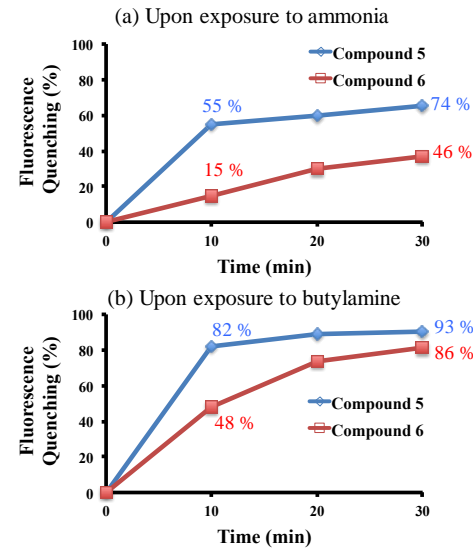


**Figure 3.** Fluorescence-quenching efficiencies of thin-layer films prepared from complexes **5** and **6** upon exposure to saturated vapors of ammonia and butylamine.

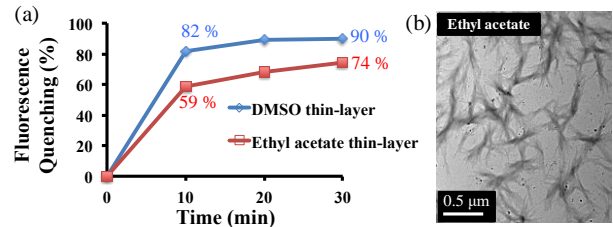


**Figure 4.** (a) Fluorescence quenching efficiencies of thin-layers prepared from DMSO and ethyl acetate, when exposed to saturated butylamine vapor, (b) TEM image of sample prepared from ethyl acetate solution (2 mM) of **5**.

Thin-layer films were prepared by dropping DMSO and ethyl acetate solutions of **5**, and their fluorescence-quenching efficiencies with butylamine were studied (Figure 4a). Complex **5** could gel DMSO but not ethyl acetate (see Table 1). The fluorescence-quenching efficiencies of the thin-layer film prepared from a warm DMSO solution were 82% and 93% after 10 and 30 min, respectively; whereas those of the thin-layer film prepared from the ethyl acetate solution were limited to 59% and 82%. The efficiency of the quenching of the thin-layer film prepared from the ethyl acetate solution of **5** was as low as that of **6**. Figure 4b shows a TEM image of a dry sample prepared from an ethyl acetate solution (2 mM; 4.48 g L<sup>-1</sup>) of complex **5**, which shows short and wide plate-like fibers with widths of ~50 nm. The short and wide plate-like fibers contrasted with the juxtaposed and interlocked fibers observed in a xerogel prepared from a warm DMSO solution (see Figure 2a).

The sensing abilities of thin-layer films were studied with saturated vapors of various amines. When a thin layer (thickness ~165 nm) prepared from a DMSO solution of complex **5** was used as a fluorescent sensor for detecting hexylamine, the quenching efficiencies were 94% and 96% after exposure for 20 and 30 min, respectively (Figure S3). The fluorescence-quenching of thin layers of complex **5** upon exposure to saturated vapors of ammonia, methylamine, butylamine,

hexylamine, aniline, and 1-naphthylamine for different time periods is shown in Figure 5a, where the thin-layer films were prepared by dropping 3  $\mu$ L of 1.0 mM DMSO solution. Note the vapor pressures for 25% ammonia solution (48.3 kPa), 40% methylamine solution (31 kPa), butylamine (10.9 kPa), hexylamine (0.866 kPa), aniline (0.04 kPa), and 1-naphthylamine (0.00053 kPa). The fluorescence-quenching efficiencies of the thin-layer films of **5** after exposure for 60 min were ~97% (hexylamine), ~93% (butylamine), ~86% (methylamine), ~74% (ammonia), ~59% (aniline), and ~40% (1-naphthylamine). These results suggest that there is no relationship between the fluorescence-quenching efficiency and the vapor pressure. The order of fluorescence-quenching efficiencies shown in Figure 5a can be explained by the basicity of amines rather than the vapor pressure. The  $pK_a$  values of hexylamine, butylamine, methylamine, ammonia, aniline, and 1-naphthylamine are 10.87, 10.77, 10.51, 9.25, 4.61, and 3.92, respectively. This order is coincident with that of the fluorescence-quenching efficiency in Figure 5a.

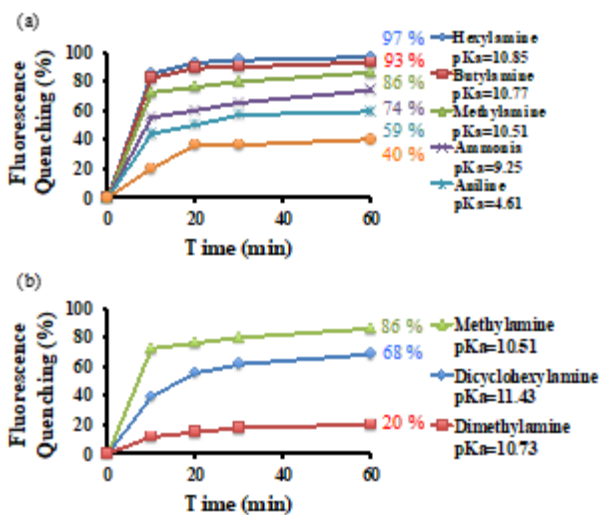


**Figure 5.** Fluorescence-quenching efficiencies by thin-layer films prepared from complex **5** upon exposure to saturated vapors of ammonia, methylamine, butylamine, hexylamine, aniline, 1-naphthylamine, methylamine, dimethylamine, and dicyclohexylamine.

Next, we studied the fluorescence-quenching after exposure to secondary amines. Figure 5b shows the fluorescence-quenching of the thin-layer films upon exposure to saturated dicyclohexylamine and dimethylamine. The fluorescence-quenching efficiencies after exposure to dicyclohexylamine and dimethylamine for 60 min were ~20% and ~68%, respectively. Considering the high basicity of dicyclohexylamine ( $pK_a = 11.43$ ) and dimethylamine ( $pK_a = 10.73$ ), the efficiencies of fluorescence-quenching by dicyclohexylamine and dimethylamine were rather low. This can be explained by taking into account the steric hindrance of secondary amines. In particular, the bulky cyclohexyl groups prevent dicyclohexylamine from coming into contact with complex **5** on the surface of the thin-layer film. It is also noteworthy that no fluorescence-quenching was observed when the film was exposed to the saturated vapor of triethylamine ( $pK_a = 10.76$ , vapor pressure = 7.2 kPa) and tributylamine ( $pK_a = 12.5$ , vapor pressure = 0.018 kPa). As a summary of the foregoing results, we concluded that (i) the efficiency of fluorescence-quenching by primary amines can be explained by their basicity; (ii) the sensitivity to secondary amines is inferior

to that to primary amines with respect to the fluorescence-quenching efficiency, and (iii) tertiary amines fail to quench the fluorescence of complex **5**. From these results, it was deduced that the fluorescence-quenching is caused by the decomposition of complex **5** on the surface of the thin-layer film; namely, nucleophilic addition of an unshared electron pair of the primary or secondary amines to the carbonyl of the  $\beta$ -diketonato group in **5** results in decomposition of the  $\text{Eu}^{3+}$  complex. Wang *et al.* reported a similar mechanism of fluorescence-quenching via nucleophilic addition of primary or secondary amines.<sup>7</sup>

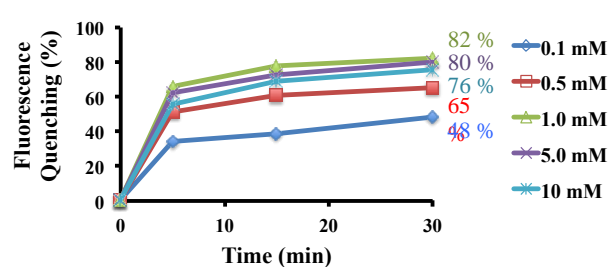


**Figure 6.** Fluorescence quenching by thin-layer films obtained from various concentrations of DMSO solutions of **5** upon exposure to saturated aniline vapor.

The relationship between the thickness of the thin-layer films and the fluorescence-quenching efficiency was investigated. The thickness of the films was determined from DFM images and the thickness was controlled by varying the concentrations of DMSO solutions of complex **5** with the drop volume fixed at 3  $\mu$ L. Although the thickness of the thin-layer film prepared from the 0.1 mM ( $0.22 \text{ g L}^{-1}$ ) solution was too thin to determine accurately, those prepared by direct drop-casting of 0.5, 1.0, 5.0, and 10 mM ( $1.12, 2.24, 5.60$ , and  $22.4 \text{ g L}^{-1}$ ) solutions were 50–60, 160–170, 200–230, and 380–400 nm, respectively. Figure 6 shows the fluorescence-quenching of thin-layer films with various thicknesses upon exposure to saturated aniline vapor. The thin-layer film prepared from the 1.0 mM solution (thickness; ~55 nm) showed the best quenching efficiency; however, the fluorescence-quenching of the thin-layer film prepared from the 10 mM solution was limited to ~76% after exposure for 30 min. The lower quenching efficiency of the film prepared from the 10 mM solution can be explained by considering the residual molecules deep within the thin-layer films, which are not quenched by exposure to aniline. Thus, we can reasonably assume that thinner films exhibit more effective fluorescence-quenching. However, it should be mentioned that when the thin-layer film is extremely thin, the fluorescence is too weak to detect. Choosing fluorescent materials having a large emission intensity may be important for sensors, because the thickness of the layers could then be reduced.

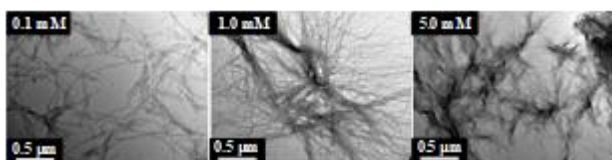


**Figure 7.** TEM images of xerogels prepared from DMSO loose gels of complex **5** at concentrations of 0.1, 1.0, and 5.0 mM.

To clarify the importance of the thickness of the thin-layer films, we measured the morphology of the aggregates by TEM. Figure 7 shows TEM images of xerogels prepared from DMSO loose gels of complex **5** at concentrations of 0.1, 1.0, and 5.0 mM.

In the image of the film prepared from the 0.1 mM solution, sparse rod-like aggregates with widths of 37–93 nm were observed. The films prepared from 1.0 and 5.0 mM solutions, which were the most appropriate concentrations for effective fluorescence-quenching, exhibited long and slender fibers that were juxtaposed and interlocked. Their widths were 19–30 nm for 1.0 mM and 37–84 nm for 5.0 mM. The wide rod-like aggregates are responsible for the lower quenching efficiency.

### 3.4. Fluorescent sensors based on 7-Eu, 7-Tb, and 7-Al

The sensing abilities of different kinds of complexes, i.e., 7-Eu, 7-Tb, and 7-Al, were studied as previously stated. The gelation abilities of 7-Tb and 7-Al are far superior to those of 5 and 7-Eu (Table 1). Figure 8 shows the efficiencies of fluorescence-quenching of thin-layer films prepared from 1.0 mM DMSO solutions of 7-Eu ( $2.49 \text{ g L}^{-1}$ ), 7-Tb ( $2.50 \text{ g L}^{-1}$ ), and 7-Al ( $2.37 \text{ g L}^{-1}$ ) by hexylamine and aniline. The efficiencies of fluorescence-quenching of 7-Tb and 7-Al reached 95 and 97% after exposure to hexylamine for 30 min, respectively (Figure 8a). The sensing abilities of 7-Tb and 7-Al are almost comparable to that of complex 5. In spite of aniline being weakly basic ( $\text{pK}_a = 4.61$ ), 7-Tb and 7-Al were so sensitive to aniline that the fluorescence-quenching efficiencies were 91 and 94%, respectively, after 30 min (Figure 8b). Considering that the efficiency of fluorescence-quenching of 5 by aniline was limited to 59% even after 60 min, the high sensitivity of 7-Tb and 7-Al was very surprising to us. Moreover, the efficiency of fluorescence-quenching of 7-Eu was substantially low, although 7-Eu was prepared from the same ligand as 7-Tb and 7-Al. To determine the reason for this, we studied the molecular packing in xerogels by WAXD. Figure 9 shows WAXD patterns for xerogels prepared from DMSO gels of 7-Eu, 7-Tb, and 7-Al. The pattern of the xerogel from 7-Eu showed four diffraction peaks corresponding to *d*-spacings of 15, 10, 7.5, and 3.8 Å, and the xerogels from 7-Tb and 7-Al exhibited broad peaks at 3.8 and 4.0 Å, respectively, indicating that the three complexes had different structures. Since the *d*-spacings of 15, 10, and 7.5 Å observed in 7-Eu fully matched the ratio of 1:2/3:1/2, it appears that a tetragonal-like aggregate was formed in the xerogel. A broad diffraction peak with a  $2\theta$  value of ~24, commonly observed in the three complexes, was ascribed to the short distance between gelator molecules within the aggregates. The low efficiency of fluorescence-quenching of the thin-layer films of 7-Eu can be explained by taking into account the low surface area of crystalline precipitates resulting from the high crystallinity.

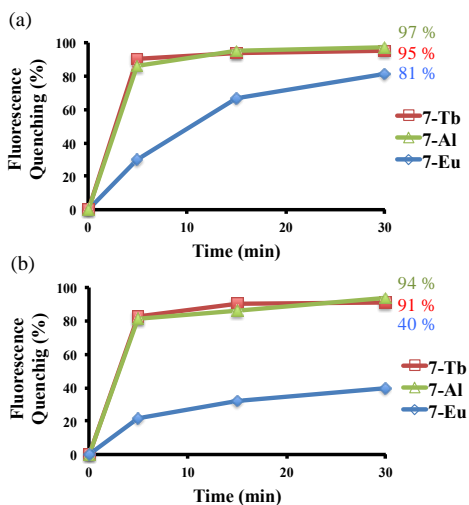


**Figure 8.** Fluorescence-quenching efficiencies by thin-layer films prepared from DMSO solutions of 7-Eu, 7-Tb, and 7-Al upon exposure to saturated vapors of (a) hexylamine and (b)

aniline.

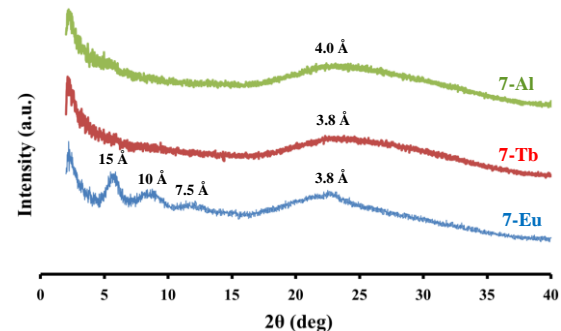


**Figure 9.** WAXD patterns for xerogels prepared from DMSO gels of 7-Eu complex, 7-Tb, and 7-Al.

Complexes 7-Tb and 7-Al exhibited high gelation abilities and could gel almost all the solvents, including DMSO, DMF, and  $\gamma$ -BL (Table 1). The effect of the solvents used to prepare the thin-layer films on the fluorescence-quenching efficiencies was studied. Figure 10 shows the efficiencies of fluorescence-quenching of thin-layer films prepared from DMSO, DMF, and  $\gamma$ -BL solutions of 7-Tb and 7-Al. The fluorescence of the thin-layer films prepared from 7-Al was effectively quenched upon exposure to saturated hexylamine vapor for 15 min (Figure 10a). When the thin-layer films prepared from 7-Tb were exposed to saturated aniline vapor with low vapor pressure and low basicity, the fluorescence-quenching efficiencies were over 90% regardless of the preparation solvents; in particular, the fluorescence of the thin-layer film prepared from a  $\gamma$ -BL solution was quantitatively quenched even after only 5 min (Figure 10b). TEM images of xerogels prepared from DMSO, DMF, and  $\gamma$ -BL solutions of 7-Tb and 7-Al revealed fibrous aggregates of juxtaposed and interlocked fibers with widths of several tens of nanometers (Figure S4).

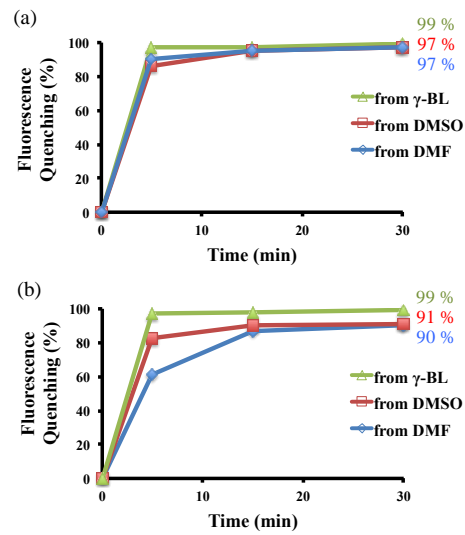


**Figure 10.** Fluorescence-quenching efficiencies by thin-layer films prepared from DMSO, DMF, and  $\gamma$ -butyrolactone solutions of 7-Tb and 7-Al.

(a) 7-Al upon exposure to saturated vapor of hexylamine.  
(b) 7-Tb upon exposure to saturated vapor of aniline.

### 3.5. Detection of tertiary amines by stimulating fluorescence emission

It is difficult to detect tertiary amines because these have

no H-atom, which is required for the nucleophilic addition and a subsequent H-elimination, and they also create steric hindrance. To the best of our knowledge, studies on solid-state sensors for detecting tertiary amines are extremely limited.<sup>6,12</sup> In practice, the fluorescence of the thin-layer films prepared from complexes **5**, **7-Eu**, **7-Tb**, and **7-Al** was not quenched when they were exposed to the vapors of tertiary amines that did not contain the H-atom required for a nucleophilic addition and a subsequent H-elimination. In order to detect tertiary amines, we conceived the idea that if the vapor of a tertiary amine reacts with  $\text{MCl}_3$  on a thin-layer film composed of  $\text{MCl}_3$  and a ligand, the corresponding complex is formed by dehydrochloric acid and then the complex generates fluorescence. With this idea in mind, thin-layer films composed of ligand **3** and europium (III) chloride hexahydrate were exposed to saturated vapors of trimethylamine, triethylamine, and tributylamine. Although the thin-layer film consisting of  $\text{EuCl}_3$  and ligand **3** was non-emissive, it transformed into a strong fluorophore after exposure to tertiary amines. Figure 11 shows the emergence of fluorescence emission followed by an increase in fluorescence intensity over time. The order of fluorescence intensity at 613 nm after exposure to amines for 30 min was triethylamine > trimethylamine > tributylamine. Given that the  $pK_a$  values of trimethylamine, triethylamine, and tributylamine are 9.75, 10.62, and 9.99, the order of fluorescence intensity can be explained by not only the basicity but also the steric hindrance of tertiary amines. It is supposed that the fluorescence emission is caused by the formation of complex **5**; when tertiary amine vapor is in contact with  $\text{EuCl}_3$  on a thin-layer film, complexation is caused by dehydrochloric acid and consequently the strongly fluorescent compound **5** is formed. The emergence of fluorescence emission and the increase in fluorescence intensity over time are the result of the formation of **5** on the thin-layer film. It is noteworthy that exposure to primary and secondary amines did not cause the emission of fluorescence from the thin-layer films consisting of  $\text{EuCl}_3$  and ligand **3**; therefore, the present thin-layer film can be characterized as a unique sensor to exclusively detect tertiary amines.

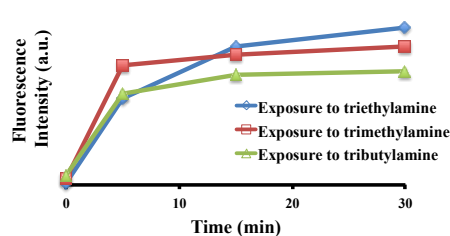


**Figure 11.** Fluorescence intensity of thin-layer films composed of ligand **3** and  $\text{EuCl}_3/6\text{H}_2\text{O}$  upon exposure to saturated vapors of trimethylamine, triethylamine, and tributylamine. Emission-monitoring wavelength was 613 nm.

#### 4. Conclusion

New compounds containing tris( $\beta$ -diketonato) complexes were prepared as fluorescent gelators that could form physical gels in some ordinary solvents. Thin-layer films were prepared on quartz plates by drop-casting solutions of metal-containing fluorescent gelators as chemosensors to detect amines. Thin-layer films were built up by fibrous aggregates of juxtaposed and interlocked fibers with widths of several tens of nanometers, and their fluorescence was effectively quenched upon exposure to saturated vapors of primary and secondary amines. The fluorescence-quenching efficiencies during the detection of primary and secondary amines were independent of the vapor

pressure of the amines and could be explained by their basicity and bulkiness. The fluorescence-quenching by primary and secondary amines was caused by decomposition of the complex through nucleophilic addition of primary or secondary amines to its carbonyl group. Thin-layer films composed of  $\text{MCl}_3$  and a ligand emitted fluorescence when they were exposed to tertiary amines. The increase in the fluorescence intensity was explained by the formation of complex **5**, which was produced by reaction with tertiary amines. These films were characterized as unique sensors to exclusively detect tertiary amines.

#### Acknowledgement

The present research was supported in part by JSPS KAKENHI Grant Number JP15K05623.

#### References

- (a) T. Gao, E. S. Tillman, N. S. Lewis, *Chem. Mater.* **2005**, *17*, 2904–2911; (b) J. M. Landete, B. Rivas, A. Marcobal, R. Muñoz, *Int. J. Food Microbiol.* **2007**, *117*, 258–269; (c) V. P. Aneja, P. A. Roelle, G. C. Murray, J. Scutherland, J. W. Erisman, D. Falter, W. A. H. Asman, N. Patni, *Atmos. Environ.* **2001**, *35*, 1903–1911; (d) P. Boeker, G. Horner, S. Rosler, *Sens. Actuators B* **2000**, *70*, 37–42; (e) T. Hernandezjover, M. Izquierdopulido, M. T. Veciananogues, M. C. Vidalcarou, *J. Agric. Food Chem.* **1996**, *44*, 2710–2715; (f) M. Nakamura, T. Sanji, M. Tanaka, *Chem. Eur. J.* **2011**, *17*, 5344–5349; (g) B. Lee, R. Scopelliti, K. Severin, *Chem. Commun.* **2011**, *47*, 9639–9641; (h) M. Loughran, D. Diamond, *Food Chem.* **2000**, *69*, 97–103; (i) E. Trevion, D. Beil, H. Steinhart, *Food Chem.* **1997**, *60*, 521–526.
- (a) J. Kumpf, S. T. Schwaebel, U. H. F. Bunz, *J. Org. Chem.* **2015**, *80*, 5159–5166; (b) J. Kumpf, J. Freudenberg, S. T. Schwaebel, U. H. F. Bunz, *Macromolecules* **2014**, *47*, 2569–2573; (c) A. Mallick, B. Garai, M. A. Addicoat, P. S. Petkov, T. Heine, R. Banerjee, *Chem. Sci.* **2015**, *6*, 1420–1425; (d) C.-F. Chow, M. H. W. Lam, W. Y. Wong, *Anal. Chem.* **2013**, *85*, 8246–8253; (e) P. Heier, N. D. Boscher, P. Choquet, K. Heinze, *Inorg. Chem.* **2014**, *53*, 11086–11095; (f) X. Pang, X. Yu, H. Lan, X. Ge, Y. Li, X. Zhen, T. Yi, *ACS Appl. Mater. Interfaces* **2015**, *7*, 13569–13577; (g) H. A. Azab, S. A. El-Korashy, Z. M. Anwar, G. M. Khairy, A. Duerkop, *J. Photochem. Photobiol. A: Chem.* **2012**, *243*, 41–46; (h) G. Giancane, V. Borovkov, Y. Inoue, L. Valli, *J. Colloid Interface Sci.* **2012**, *385*, 282–284; (i) X. J. Huang, T. Y. You, T. Li, X. R. Yang, E. K. Wang, *Electroanalysis* **1999**, *11*, 969–972; (j) Y. M. Chung, B. Raman, K. H. Ahn, *Tetrahedron* **2006**, *62*, 11645–11651; (k) X. Yang, G. Peter, C. Hauser, *Electrophoresis* **2006**, *27*, 468–473; (l) W. X. Zhang, Z. X. Chen, Z. H. Yang, *Phys. Chem. Chem. Phys.* **2009**, *11*, 6263–6268; (m) L. Feng, C. J. Musto, J. W. Kemling, S. H. Lim, K. S. Suslick, *Chem. Commun.* **2010**, *46*, 2037–2039; (n) S. Körsten, G. J. Mohr, *Chem. Eur. J.* **2011**, *17*, 969–975.
- C. Wang, X. W. He, L. X. Chen, *Talanta* **2002**, *57*, 1181–1188.
- C. J. Liu, J. T. Lin, S. H. Wang, J. C. Jiang, L. G. Lin, *Sensors and Actuators B*, **2005**, *108*, 521–527.
- S. A. Brittle, T. H. Richardson, J. Hutchinson, C. A. Hunter, *Colloids Surf. A* **2008**, *321*, 29–33.
- X. Zhang, X. Liu, R. Lu, H. Zhang, P. Gong, *J. Mater. Chem.* **2012**, *22*, 1167–1172.
- Z. Zhou, Q. Wang, J. Lin, Y. Chen, C. Yang, *Photochem. Photobiol.* **2012**, *88*, 840–843.
- Y. Fu, Q. He, D. Zhu, Y. Wang, Y. Gao, H. Cao, J. Cheng, *Chem. Commun.* **2013**, *49*, 11266–11268.

9. C. F. Chow, M. H. W. Lam, W. Y. Wong, *Anal. Chem.* **2013**, *85*, 8246–8253.
10. P. Xue, Q. Xu, P. Gong, C. Qian., A. Ren, Y. Zhang, R. Lu, *Chem. Commun.* **2013**, *49*, 5838–5840.
11. T. Han, J. W. Y. Lam, N. Zhao, M. Gao, Z. Yang, E. Zhao, Y. Dong, B. Z. Tang, *Chem. Commun.* **2013**, *49*, 4848–4850.
12. S. Rochat, T. M. Swager, *Angew. Chem. Int. Ed.* **2014**, *53*, 9792–9796.
13. J. Kumpf, J. Freudenberg, K. Fletcher, A. Dreuw, U. H. F. Bunz, *J. Org. Chem.* **2014**, *79*, 6634–6645.
14. J. Yao, Y. Fu, W. Fan, Q. He, D. Zhu, H. Cao, J. Cheng, *RSC Adv.* **2015**, *5*, 25125–25131.
15. K. Hanabusa, M. Suzuki, *Bull. Chem. Soc. Jpn.* **2016**, *89*, 174–182.
16. K. Hanabusa, K. Harano, M. Fujisaki, Y. Nomura, M. Suzuki, *Macromolecular Sympo.* **2016**, *364*, 7–8.
17. K. Hanabusa, S. Takata, M. Fujisaki, Y. Nomura, M. Suzuki, *Bull. Chem. Soc. Jpn.* **2016**, *89*, 1391–1401.
18. (a) ed. F. Fages, *Low Molecular Mass Gelators; Design, Self-Assembly, Function* Springer, Berlin Heidelberg New York, **2005**; (b) P. Dastidar, *Chem. Soc. Rev.* **2008**, *37*, 2699–2715; (c) S. Banerjee, R. K. Das, U. Maitra, *J. Mater. Chem.* **2009**, *19*, 6649–6687; (d) M. Suzuki, K. Hanabusa, *Chem. Soc. Rev.* **2009**, *38*, 967–975; (e) M. Suzuki, K. Hanabusa, *Chem. Soc. Rev.* **2010**, *39*, 455–463; (f) J. L. Li, X. Y. Liu, *Adv. Funct. Mater.* **2010**, *20*, 3196–3216; (g) G. John, B. V. Shankar, S. R. Jadhav, P. K. Vemula, *Langmuir* **2010**, *26*, 17843–17851; (h) H. Svobodová, V. Noponen, E. Kolehmainen, E. Sievänen, *RSC Adv.* **2012**, *2*, 4985–5007; (i) S. S. Babu, S. Prasanthkumar, A. Ajayaghosh, *Angew. Chem., Int. Ed.* **2012**, *51*, 1766–1776; (j) A. Y. Y. Tam, V. W. W. Yam, *Chem. Soc. Rev.* **2013**, *42*, 1540–1567; (k) J. Raeburn, A. Z. Cardoso, D. J. Adams, *Chem. Soc. Rev.* **2013**, *42*, 5143–5156; (l) G. Yu, X. Yan, C. Han, F. Huang, *Chem. Soc. Rev.* **2013**, *42*, 6697–6722; (m) M. D. Segarra-Maset, V. J. Nebot, J. F. Miravet, B. Escuder, *Chem. Soc. Rev.* **2013**, *42*, 7086–7098; (n) S. S. Babu, V. K. Praveen, A. Ajayaghosh, *Chem. Rev.* **2014**, *114*, 1973–2129; (o) D. K. Kumar, J. W. Steed, *Chem. Soc. Rev.* **2014**, *43*, 2080–2088; (p) V. K. Praveen, C. Ranjith, N. Armaroli, *Angew. Chem., Int. Ed.* **2014**, *53*, 365–368; (q) Y. Lan, M. G. Corradinia, R. G. Weiss, S. R. Raghavanc, M. A. Rogers, *Chem. Soc. Rev.* **2015**, *44*, 6035–6058; (r) K. Hanabusa, *Polym. J.* **2014**, *46*, 776–782.

## Graphical Abstract

<Title>

Detection of Amine Vapors using Luminescent Xerogels from Supramolecular Metal-Containing Gelator

<Authors' names>

Junpei Sasaki, Masahiro Suzuki, Kenji Hanabusa

<Summary>

Fluorescent gelators containing a tris( $\beta$ -diketonato) complex are synthesized by using gelation-driving chelates, and their gelation abilities are studied. Thin-layer films are prepared on quartz plates from the solutions and studied as chemosensors for amines. The fluorescence-quenching efficiencies upon exposure to saturated primary and secondary amines depend on the basicity and bulkiness of the amines rather than the vapor pressure.

<Diagram>

